ISSN 1674-1056
http://cpb.iphy.ac.cn
http://iopscience.iop.org/cpb
中国物理 B
Chinese Physics
中国物理
Chinese Physics B

A novel multi-scroll chaotic generator:Analysis, simulation and implementation

Gui-Tao Zhang(张桂韬), Fa-Qiang Wang(王发强)
Citation: Chin. Phys. B . 2018, 27(1): 018201. **doi:** 10.1088/1674-1056/27/1/018201

Journal homepage: http://cpb.iphy.ac.cn; http://iopscience.iop.org/cpb

What follows is a list of articles you may be interested in

Bursting oscillations in a hydro-turbine governing system with two time scales

Qing-Shuang Han(韩青爽), Di-Yi Chen(陈帝伊), Hao Zhang(张浩)
Chin. Phys. B . 2017, 26(12): 128202. **doi:** 10.1088/1674-1056/26/12/128202

Numerical simulation and analysis of complex patterns in a two-layer coupled reaction diffusion system

Li Xin-Zheng, Bai Zhan-Guo, Li Yan, He Ya-Feng, Zhao Kun
Chin. Phys. B . 2015, 24(4): 048201. **doi:** 10.1088/1674-1056/24/4/048201

Nonlinear dynamic characteristics and optimal control of a giant magnetostrictive film-shaped memory alloy composite plate subjected to in-plane stochastic excitation

Zhu Zhi-Wen, Zhang Qing-Xin, Xu Jia
Chin. Phys. B . 2014, 23(8): 088201. **doi:** 10.1088/1674-1056/23/8/088201

A voltage-controlled chaotic oscillator based on carbon nanotube field-effect transistor for low-power embedded systems

Van Ha Nguyen, Wonkyeong Park, Namtae Kim, Hanjung Song
Chin. Phys. B . 2014, 23(5): 058201. **doi:** 10.1088/1674-1056/23/5/058201

Effect of metal oxide arrester on the chaotic oscillations in the voltage transformer with nonlinear core loss model using chaos theory

Hamid Reza Abbasi, Ahmad Gholami, Seyyed Hamid Fathi, Ataollah Abbasi
Chin. Phys. B . 2014, 23(1): 018201. **doi:** 10.1088/1674-1056/23/1/018201

A novel multi-scroll chaotic generator: Analysis, simulation, and implementation*

Gui-Tao Zhang (张桂韬) and Fa-Qiang Wang(王发强)†

State Key Laboratory of Electrical Insulation and Power Equipment, School of Electrical Engineering, Xi'an Jiaotong University, Xi'an 710049, *China*

(Received 6 August 2017; revised manuscript received 16 October 2017; published online 28 November 2017)

Based on a new three-dimensional autonomous linear system and designing a specific form of saturated function series and a sign function with two variables of system, which are employed to increase saddle-focus equilibrium points with index 2, a novel multi-scroll chaotic system is proposed and its typical dynamical characteristics including bifurcation diagram, Poincare map, and the stability of equilibrium points are analyzed. The hardware circuit is designed and the experimental results are presented for confirmation.

Keywords: multi-scroll chaotic system, linear system, hardware circuit

PACS: 82.40.Bj **DOI:** 10.1088/1674-1056/27/1/018201

1. Introduction

Lorenz[7] found the first classical chaotic system in 1963, which is a cornerstone laid for scholars to study chaos and its applications. Chaos, which is the complex motion of nonlinear dynamical system, has been widely found and accepted in biology,[1] chemistry,[2] engineering,[3] social sciences,[4] and other fields of science.[5,6] Especially, in the field of electronic circuits, since the typical Chua circuit[8] was presented in 1984, it has quickly become a paradigm to research chaos and a bridge between electronic circuits and the chaos theory.[9–11] It has a sound engineering application background and lays the foundation for the development of a multi-scroll and multi-wing chaotic system. In the last few decades, multi-scroll or multi-wing chaotic systems have been proposed and some kinds of topologies and shapes of the multi-scroll or multi-wing chaotic attractors have been reported in the literature.[12–26] For example, Suykens et al. introduced a quasilinear approach to generating n-double scrolls ($n = 1, 2, 3, \ldots$).[16] Yalcin *et al.* presented families of scroll grid attractors including one-dimensional (1D)-grid scroll, two-dimensional (2D)-grid scroll, three-dimensional (3D)-grid scroll attractors with step functions.[21] Tang *et al.* employed a sine function for generating n-scroll attractors in a simple circuit.[18] Lü *et al.* presented a switching manifold approach to generating chaotic attractors with multiple merged basins of attraction.[25] Also, Lü *et al.* introduced the hysteresis and saturated functions series methods to generate multi-scroll chaotic attractors with rigorous mathematical proof and physical realization for the chaotic behaviors.[22,23] Yu *et al.* presented a general jerk circuit for creating various types of multi-scroll chaotic attractors.[24] As indicated in Ref. [20], compared with conventional simple chaotic system, the multi-scroll or multi-wing chaotic system has a complicated topological structure, so that it is a good candidate for fingerprint images encryption,[27] digital secure communications,[28] entropy of a random number generator,[29] etc.[30,31] Therefore, it is very important and valuable to explore the novel multi-scroll or multi-wing chaotic systems. In this paper, based on a new simple three-dimensional linear system and designing a specific form of saturated function series and a step function with two variables of system, which are employed to increase saddle-focus equilibrium points with index 2, a novel multi-scroll chaotic system is constructed. Both simulation results and hardware circuit implementation are presented for confirmation.

The rest of this paper is organized as follows. In Section 2, a novel multi-scroll chaotic system is presented. The dynamical characteristics of the novel multi-scroll chaotic system are investigated in Section 3. In Section 4, the hardware circuit is designed, and the experimental results are in good agreement with the numerical simulation. Finally, some conclusions are drawn from the present study in Section 5.

2. A novel multi-scroll chaotic system

As is well known, a chaotic system which is a nonlinear system in nature possesses local instability around one or more equilibrium points. This local instability can be identified by linearizing the chaotic system around its equilibrium point to

*Project supported by the National Natural Science Foundation of China (Grant Nos. 51377124 and 51521065), the Foundation for the Author of National Excellent Doctoral Dissertation, China (Grant No. 201337), and the New Star of Youth Science and Technology of Shaanxi Province, China (Grant No. 2016KJXX-40).

†Corresponding author. E-mail: faqwang@mail.xjtu.edu.cn

© 2018 Chinese Physical Society and IOP Publishing Ltd

obtain its corresponding linear system, which is easy to judge its stability. Accordingly, this linear system is a key part for constructing the chaotic system.

A novel simple 3D linear system is described by

$$\begin{cases} \dot{x} = 303.03(y+z), \\ \dot{y} = az, \\ \dot{z} = -90.70(x+y+z), \end{cases} \tag{1}$$

where a is the parameter of system (1). Apparently, $S_0 = (0,0,0)$ is the origin of system (1) and its characteristic equation is given by

$$\lambda^3 + 90.70\lambda^2 + 90.70 \times (303.03 + a)\lambda + 90.70 \times 303.03 \times a = 0. \tag{2}$$

According to the Routh–Hurwitz criterion, when $a > 129.44$, equation (2) has one negative real root and two complex conjugate roots with a positive real part. It is demonstrated that system (2) becomes unstable when a satisfies the condition of $a > 129.44$ and $S_0 = (0,0,0)$ is a saddle-foci point of index 2.

In order to generate multi-scroll chaotic attractors, the main design idea is to introduce additional saddle-focus points by adding some additional breakpoints in the proposed system. Here, a novel multi-scroll chaotic system based on the above simple three-dimensional linear system is constructed by introducing a saturated function series and a special step function with two variables of system.

Accordingly, the novel multi-scroll chaotic system can be expressed as follows:

$$\begin{cases} \dot{x} = 303.03(y+z-g_K(y)), \\ \dot{y} = az, \\ \dot{z} = -90.70(x+y+z-h(x+y)), \end{cases} \tag{3}$$

where

$$g_K(y) = \sum_{k=-K}^{K} \frac{A}{2\alpha}\left[|y-2kA+\alpha| - |y-2kA-\alpha|\right], \tag{4}$$

$$h(x+y) = b\,\mathrm{sgn}(x+y), \tag{5}$$

a, b are parameters and x, y, z are variables of the system (3). In Eq. (4), $g_K(y)$ is one form of saturated function series, K is a positive integer, $A > 0$, $\alpha \in (0, A)$, and $A/\alpha > 1$. Therefore, the saturated slope and turning points of the saturated function series are A/α and $2kA \pm \alpha$ ($k = 0, \pm1, \pm2, \ldots, \pm K$), respectively. For $K = 3$, the saturated function series of Eq. (4) is shown in Fig. 1. In Eq. (5), $h(x+y)$ can be described as follows:

$$h(x+y) = \begin{cases} b, & x+y > 0, \\ 0, & x+y = 0, \\ -b, & x+y < 0, \end{cases} \tag{6}$$

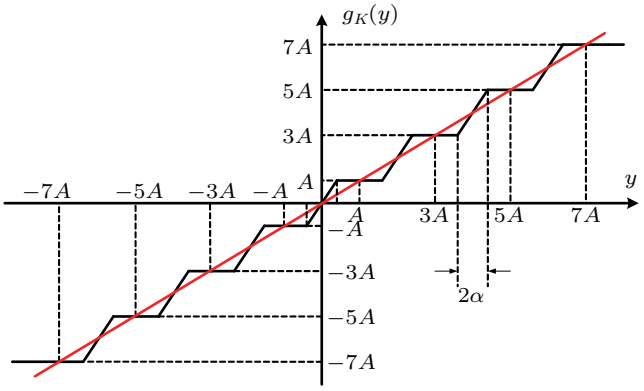


Fig. 1. Saturated function series when $K = 3$.

System (3) can generate $(2K+2) \times 2$-scroll chaotic attractors when $a > 129.44$ is selected. Setting the initial condition $(x_0, y_0, z_0) = (1, 1, 1)$, the simulation results from Matlab software can be obtained and shown in Figs. 2 and 3. One can see that system (3) can generate 4-scroll, 8-scroll, and 24-scroll chaotic attractors, when $K = 0$, $K = 1$, and $K = 5$ are selected. Hence, it is effective to use the above method to generate multi-scroll chaotic attractors.

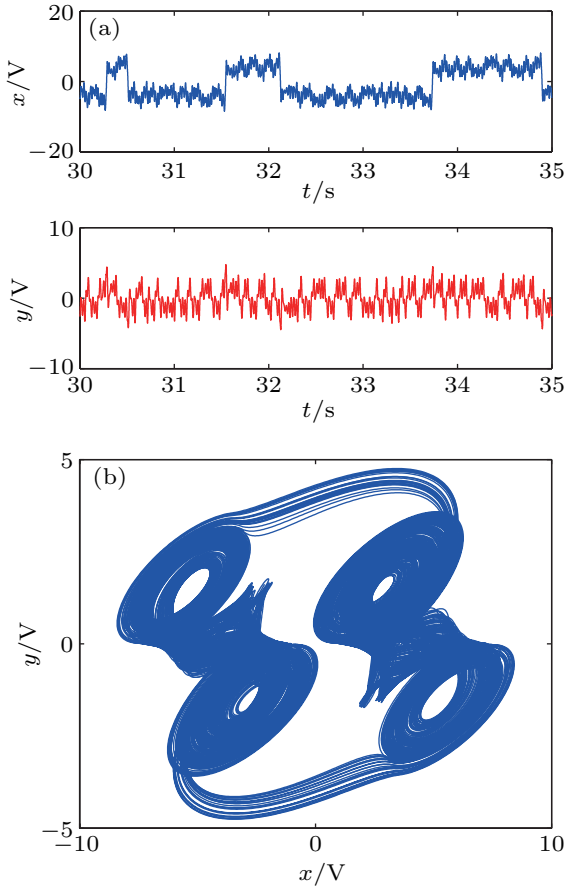


Fig. 2. (color online) 4-scroll chaotic attractors for $A = 1.55$, $\alpha = 0.03$, $a = 303.03$, $b = 4.18$, $K = 0$: (a) x and y; (b) x–y.

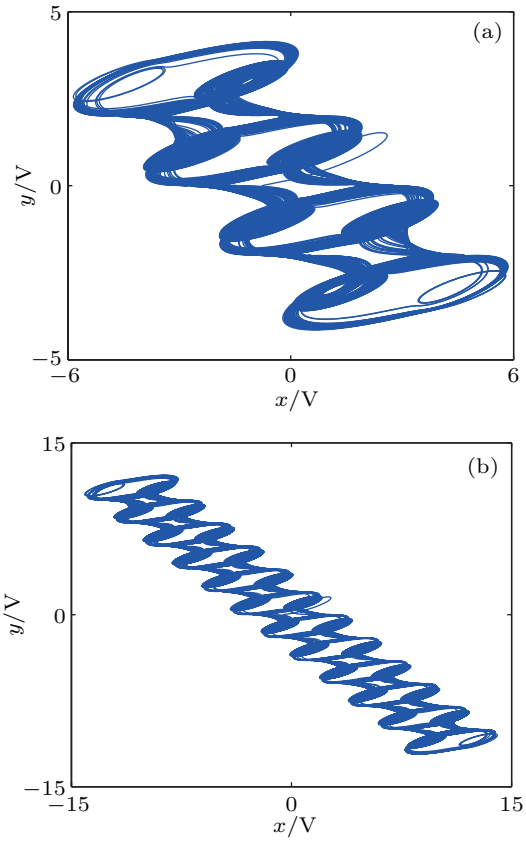


Fig. 3. (color online) $(2K+2)\times 2$-scroll chaotic attractors for $A=1$, $\alpha=0.02$, $b=1.58$: (a) 8-scroll attractor ($a=183.03$, $K=1$); (b) 24-scroll attractor ($a=190.03$, $K=5$).

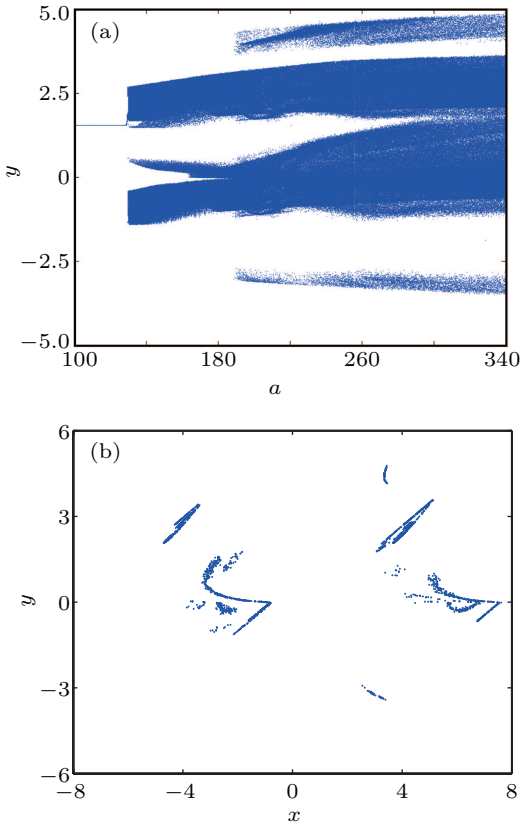


Fig. 4. (color online) Dynamical properties of system (3): (a) bifurcation diagram; (b) Poincare map on the x–y phase plane with $z=0$, $a=303.03$.

3. Dynamical characteristics of novel multi-scroll chaotic system

In this section, the dynamical characteristics of the novel multi-scroll chaotic system (3) including bifurcation diagram, Poincare map, and equilibrium points are illustrated.

3.1. Bifurcation diagram and Poincare map

Let $A=1.55$, $\alpha=0.03$, $b=4.18$, $K=0$ and the initial condition $(x_0, y_0, z_0)=(1,1,1)$. The bifurcation diagram which corresponds to the state variable y changing with parameter a is shown in Fig. 4(a). For $a\in(100,340)$, one can see that as a increases, bifurcation occurs at the point $a=129.44$. In Fig. 4(b), a Poincare map is also given to further observe the dynamical behaviors of the system. The Poincare map is rendered as patches of dense points, and shows that the system is chaotic.

3.2. Equilibrium points and its stability

Let the terms on the right-hand side of system (3) be equal to zero, then the following equations will be obtained:

$$\begin{cases} y+z-g_K(y)=0, \\ az=0, \\ -90.70(x+y+z-h(x+y))=0. \end{cases} \tag{7}$$

Then, $z=0$, $y-g_K(y)=0$, and $x+y-h(x+y)=0$. Clearly, system (3) has $((2K+2)\times 2+(2K+1)\times 2)$ equilibrium points. Here, it should be pointed out that there are two kinds of equilibrium points: ${}^{\mathrm{E}}S$ ($y^*=2kA$, ($k=0,\pm1,\pm2,\ldots,\pm N$)) and ${}^{\mathrm{O}}S$ ($y^*=2(k-1)A$, ($k=0,\pm1,\pm2,\ldots,\pm N$)). At the equilibrium points $S^*=(x^*,y^*,z^*)$, the Jacobian matrix of system (3) is given by

$$J=\begin{bmatrix} 0 & 303.03(1-g'_K(y^*)) & 303.03 \\ 0 & 0 & a \\ -90.70 & -90.70 & -90.70 \end{bmatrix}, \tag{8}$$

where $g'_K(y^*)=\mathrm{d}g_K(y)/\mathrm{d}y|y^*$ and the derivative of Eq. (4) at y^* is evaluated by

$$\mathrm{d}g_K(y)/\mathrm{d}y|y^* = \sum_{k=-K}^{K}\frac{A}{2\alpha}[\mathrm{sgn}(y^*-2kA+\alpha) - \mathrm{sgn}(y^*-2kA-\alpha)]. \tag{9}$$

If $y^*=2kA$, ($k=0,\pm1,\pm2,\ldots,\pm K$), then $g'_K(y^*)=A/\alpha$; else if $y^*=2(k-1)A$, ($k=0,\pm1,\pm2,\ldots,\pm K$), then$g'_K(y^*)=0$. Linearization of the system around S^* yields the following characteristic equation:

$$\lambda^3+90.70\lambda^2+90.70\times(303.03+a)\lambda +90.70\times 303.03\times(1-g'_K(y^*))\times a=0. \tag{10}$$

For ${}^{\mathrm{E}}S$ ($y^* = 2kA$, ($k = 0, \pm1, \pm2, \ldots, \pm K$)), then $g'_K(y^*) = A/\alpha$. Equation (10) can be reduced to

$$\lambda^3 + 90.70\lambda^2 + 90.70 \times (303.03 + a)\lambda + 90.70 \times 303.03 \times (1 - A/\alpha) \times a = 0. \quad (11)$$

For $a < 90.70/(1 - A/\alpha - 90.70/303.03)$, equation (11) has one negative real root and two complex conjugate roots with positive real part so that all equilibrium points ${}^{\mathrm{E}}S$ are unstable saddle-foci.

For ${}^{\mathrm{O}}S$ ($y^* = 2(k-1)A$, $k = 0, \pm1, \pm2, \ldots, \pm K$), then $g'_K(y^*) = 0$. Equation (10) is similar to Eq. (2). As a result, when $a > 129.44$, equation (10) has one negative real root and two complex conjugate roots with positive real part so that all equilibrium points ${}^{\mathrm{O}}S$ are also unstable saddle-foci.

Let $A = 1.55$, $\alpha = 0.03$, $b = 4.18$, $K = 0$, and $a = 303.03$, then system (3) will have only 4 equilibrium points being ${}^{\mathrm{O}}S$ and three roots of ${}^{\mathrm{O}}S$ will be $\lambda_1 = 22.74 + 246.26\mathrm{i}$, $\lambda_2 = 22.74 - 246.26\mathrm{i}$, and $\lambda_3 = -136.17$; let $A = 1.55$, $\alpha = 0.03$, $b = 4.18$, $K = 0$, and $a = -303.03$ ($-303.03 < 90.70/(1 - 1.55/0.03 - 90.70/303.03)$), then system (3) will have only 4 equilibrium points being ${}^{\mathrm{E}}S$ and three roots of ${}^{\mathrm{E}}S$ will have $\lambda_1 = 345.43 + 648.55\mathrm{i}$, $\lambda_2 = 345.43 - 648.55\mathrm{i}$, and $\lambda_3 = -781.55$. In these two cases, although all the equilibrium points are saddle points of index 2, the scrolls of the chaotic attractors can emerge only from ${}^{\mathrm{O}}S$ (when $a = 303.03$). So it can be deduced that the values of ${}^{\mathrm{O}}S$ are real while the values of ${}^{\mathrm{E}}S$ are virtual in the system. Hence, for $a > 129.44$, the $(2K+2) \times 2$-scroll chaotic attractors can be generated.

4. Circuit design and experimental results

According to Eq. (3) and Fig. 2, the hardware circuit is designed to have three parts: a main circuit as shown in Fig. 5(c), which has two input ports ($0.39h(x+y)$, $-g_K(y)$) and three output ports ($-0.39y$, y, $-0.39x$); a circuit for obtaining function $h(x+y)$ (Fig. 5(a)), which has two input ports ($-0.39x$, $-0.39y$) and one output port $0.39h(x+y)$; a circuit for obtaining function $g_K(y)$ (Fig. 5(b)), which has one input port (y) and one output port ($-g_K(y)$). All the operational amplifiers used in the circuits are all AD711 whose power supplies are ±17 V. It should be noted that (i) when the power supplies of AD711 are ±17 V, its saturation output voltage measured in the experimental setup is ±17 V; (ii) in Fig. 5(b),

$$\alpha = \frac{R_6 |E_{\mathrm{sat}}|}{R_5} = \frac{1\ \mathrm{k} \times |\pm 17|}{620\ \mathrm{k}} \approx 0.03,$$
$$\frac{A}{\alpha} = \frac{620\ \mathrm{k}}{1\ \mathrm{k}} \times \frac{1\ \mathrm{k}}{12\ \mathrm{k}} \approx 51.67.$$

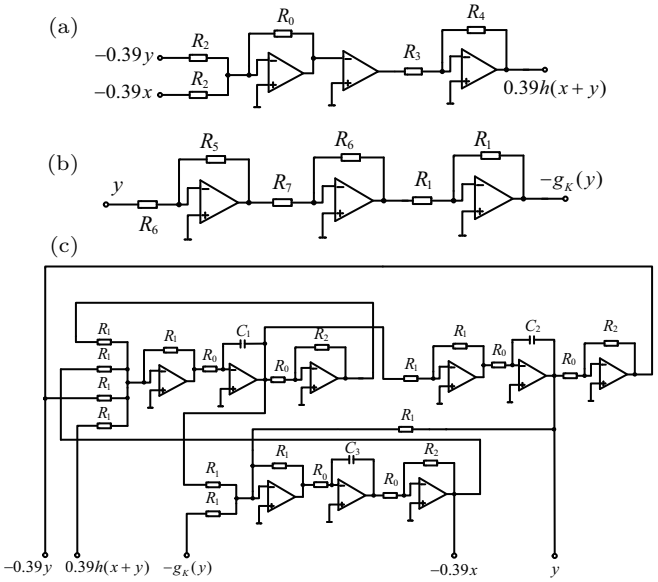


Fig. 5. Experimental circuit: (a) circuit for obtaining function $h(x+y)$; (b) circuit for obtaining function $g_K(y)$; (c) main circuit.

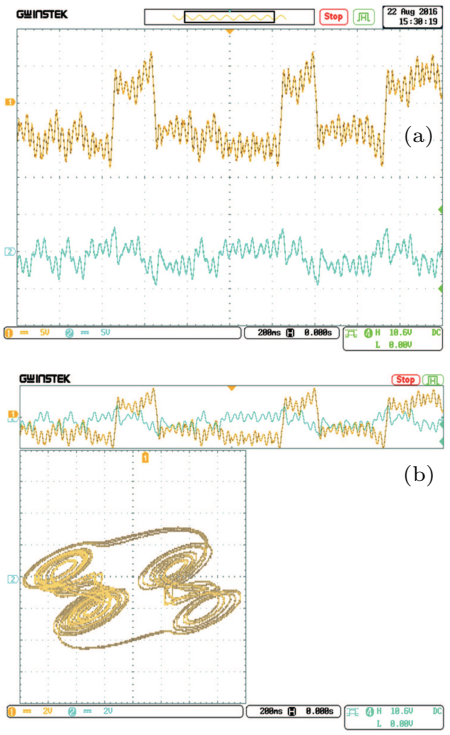


Fig. 6. (color online) Experimental results observed from practical circuits for generating 4-scroll chaotic attractor with $A = 1.55$, $\alpha = 0.03$, $a = 303.03$, $b = 4.18$, and $K = 0$: (a) time domain diagram of t–x and t–y; (b) the phase diagram of system (3) on the x–y phase plane.

Connect the input and output ports of the designed circuits, then the following equations will be obtained:

$$\begin{cases} \dot{x} = \dfrac{1}{R_0 C_3}(y + z - g_K(y)), \\ \dot{y} = \dfrac{1}{C_2 R_0} z, \\ \dot{z} = -\dfrac{R_2}{C_1 R_0^2}\left(x + y + z - \dfrac{R_0 R_4 |E_{\mathrm{sat}}|}{R_2 R_3}\mathrm{sgn}(x+y)\right), \\ g_K(y) = \dfrac{R_5}{2R_7}\left[\left|y + \dfrac{R_6 |E_{\mathrm{sat}}|}{R_5}\right| - \left|y - \dfrac{R_6 |E_{\mathrm{sat}}|}{R_5}\right|\right]. \end{cases} \quad (12)$$

So

$$\frac{1}{R_0C_3}=303.03,\quad \frac{R_5}{2R_7}=\frac{A}{2\alpha},\quad \frac{R_6\,|E_{\rm sat}|}{R_5}=\alpha,$$
$$\frac{1}{C_2R_0}=a,\quad -\frac{R_2}{C_1R_0^2}=-90.70,\quad \frac{R_0R_4\,|E_{\rm sat}|}{R_2R_3}=b.$$

Taking $R_0=100$ k, $R_1=10$ k, $R_2=39$ k, $R_3=120$ k, $R_4=11.5$ k, $R_5=620$ k, $R_6=1$ k, $R_7=12$ k, $C_1=43$ nF, $C_2=C_3=33$ nF, the experimental results can be observed from the digital oscilloscope GDS3254 and shown in Fig. 6. Comparing Fig. 6 with Fig. 2, one can see that they are in good agreement with each other.

5. Conclusions

In this paper, based on a new 3D autonomous linear system, a novel $(2K+2)\times 2$-scroll chaotic attractor is constructed by introducing a specific form of saturated function series and a step function with two variables of system to increase saddle-focus equilibrium points with index 2. The theoretical analysis, Matlab simulations and circuit experiments are in good agreement with each other and all of them show that this novel multi-scroll chaotic system can generate $(2K+2)\times 2$-scroll chaotic attractors. What is more important is that other novel multi-scroll chaotic topologies can be easily obtained by changing the relationship between the two variables of the system. For example, if $h(x+y)$ which is used here are changed into $h(x-y)$, $h(y+z)$ or other relationships, one can obtain other quite different novel multi-scroll chaotic attractors.

References

[1] Misteli T 2008 *Nature* **456** 333
[2] Cramer J A and Booksh K S 2006 *J. Chemom.* **20** 447
[3] Hirata Y, Oku M and Aihara K 2012 *Chaos* **22** 047511
[4] Murphy P 1996 *Public Relat. Rev.* **22** 95
[5] Kerr R A 2007 *Science* **317** 449
[6] Oxley L and George D A R 2007 *Environ. Model. Softw.* **22** 580
[7] Lorenz E 1963 *J. Atmos. Sci.* **20** 130
[8] Matsumoto T 1984 *IEEE Trans. Circuits Syst.* **31** 1055
[9] Chen G and Ueta T 1999 *Int. J. Bifurc. Chaos* **9** 1465
[10] Lü J Chen G 2002 *Int. J. Bifurc. Chaos* **12** 659
[11] Lü J, Chen G, Chen D and Celikovsky S 2002 *Int. J.Bifurc. Chaos* **12** 2917
[12] Wang C H, Xu H and Yu F 2013 *Int. J. Bifurc. Chaos* **23** 1350022
[13] Zhang CX and Yu S M 2010 *Phys. Lett. A* **374** 3029
[14] Lü J H, Murali K, Sinha S, Leung H and Aziz-Alaoui M A 2008 *Phys. Lett. A* **372** 3234
[15] Wang X Y, Lin D and Wang Z J 2009 *Phys. Lett. B* **23** 2021
[16] Suykens J A K and Vandewalle J 1993 *IEEE Trans. Circuits Syst. I* **40** 861
[17] Luo X H, Tu Z W, Liu X R, Cai C, Liang Y L and Gong P 2010 *Chin. Phys. B* **19** 070510
[18] Tang W K S, Zhong G Q, Chen, G and Man K F 2001 *IEEE Trans. Circuits Syst. I* **48** 1369
[19] Lü J and Chen G 2006 *Int. J. Bifurc. Chaos* **16** 775
[20] Wang Z H, Qi G Y, Sun Y X, van Wyk B J and van Wyk M A 2010 *Nonlinear Dyn.* **60** 443
[21] Yalcin M E, Suykens J A K, Vandewalle J and Ozoguz S 2002 *Int. J. Bifurc. Chaos* **12** 23
[22] Lü J H, Chen G R, Yu X H and Leung H 2004 *IEEE Trans. Circuits Syst. I* **51** 2476
[23] Lü J H, Yu S M, Leung H and Chen G R 2006 *IEEE Trans. Circuits Syst. I* **53** 149
[24] Yu S M, Lü J H, Leung H and Chen G R 2005 *IEEE Trans. Circuits Syst. I* **52** 1459
[25] Lü J H, Yu X H and Chen G R 2003 *IEEE Trans. Circuits Syst. I* **50** 198
[26] Wang F Q and Liu C X 2007 *Chin. Phys.* **16** 1009
[27] Han F, Hu J, Yu X and Wang Y 2007 *Appl. Math. Comput.* **185** 931
[28] Tang K S, Man K F and Chen G 2001 *Proc. IEEE Int. Symp. Circ. Syst.* **3** 787
[29] Yalcin M E 2007 *Int. J. Bifurc. Chaos* **17** 4471
[30] Gamez-Guzman L, Cruz-Hernandez C, Lopez-Gutierrez R and Garcia-Guerrero E E 2009 *Commun. Nonlinear Sci. Numer. Simul.* **14** 2765
[31] Yalcin M E, Suykens J A K and Vandewalle J 2004 *Proc. IEEE Int. Symp. Circ. Syst.* **4** 581